

Swi/Snf chromatin remodeling/tumor suppressor complex establishes nucleosome occupancy at target promoters

Michael Y. Tolstorukov^{a,b,1,2}, Courtney G. Sansam^{c,d,e,1}, Ping Lu^{c,d,e,1}, Edward C. Koellhoffer^{c,d,e}, Katherine C. Helming^{c,d,e}, Burak H. Alver^a, Erik J. Tillman^{c,d,e}, Julia A. Evans^{c,d,e}, Boris G. Wilson^{c,d,e}, Peter J. Park^{a,b,3}, and Charles W. M. Roberts^{c,d,e,3}

^aCenter for Biomedical Informatics, Harvard Medical School, Boston, MA 02115; ^bDivision of Genetics, Brigham and Women's Hospital, Boston, MA 02115; ^cDepartment of Pediatric Oncology, Dana-Farber Cancer Institute, Boston, MA 02115; ^dDivision of Hematology/Oncology, Boston Children's Hospital, Boston, MA 02115; and ^eDepartment of Pediatrics, Harvard Medical School, Boston, MA 02115

Edited by Mark Groudine, Fred Hutchinson Cancer Research Center, Seattle, WA, and approved May 2, 2013 (received for review February 6, 2013)

Precise nucleosome-positioning patterns at promoters are thought to be crucial for faithful transcriptional regulation. However, the mechanisms by which these patterns are established, are dynamically maintained, and subsequently contribute to transcriptional control are poorly understood. The switch/sucrose non-fermentable chromatin remodeling complex, also known as the Brg1 associated factors complex, is a master developmental regulator and tumor suppressor capable of mobilizing nucleosomes in biochemical assays. However, its role in establishing the nucleosome landscape in vivo is unclear. Here we have inactivated Snf5 and Brg1, core subunits of the mammalian Swi/Snf complex, to evaluate their effects on chromatin structure and transcription levels genome-wide. We find that inactivation of either subunit leads to disruptions of specific nucleosome patterning combined with a loss of overall nucleosome occupancy at a large number of promoters, regardless of their association with CpG islands. These rearrangements are accompanied by gene expression changes that promote cell proliferation. Collectively, these findings define a direct relationship between chromatin-remodeling complexes, chromatin structure, and transcriptional regulation.

In eukaryotic cells, DNA is tightly wrapped around a core of histone proteins to form nucleosomes, the basic units of chromatin structure. Because nucleosomes can impede transcription factors binding to DNA, dynamic regulation of nucleosome positioning is thought to play a critical role in transcriptional control and, in turn, numerous biological processes. Consequently, elucidating the mechanisms that modulate chromatin structure has been of great interest and has the potential to provide fundamental insight into the control of gene regulation.

Nucleosomes are assembled, modified, and repositioned with the assistance of chromatin remodeling complexes. Two broad classes of such complexes are known: those that covalently modify histones and those that use the energy of ATP hydrolysis to mobilize nucleosomes and remodel chromatin. The Swi/Snf complex was one of the first chromatin remodeling complexes to be identified, with many of its subunits conserved from yeast to humans. In mammalian cells, the Swi/Snf complex comprises 11–15 protein subunits that include SNF5 (SMARCB1) and one of the two mutually exclusive ATPases, BRG1 (SMARCA4) or BRM (SMARCA2) (1–3). The Swi/Snf complex is capable of facilitating both gene activation and repression and contributes to the regulation of lineage specificity and cell fate determination (4, 5).

Growing evidence indicates that the Swi/Snf complex serves a widespread role in tumor suppression. *SNF5* was the first subunit linked to cancer and is inactivated in nearly all childhood malignant rhabdoid tumors as well as some cases of familial schwannomatosis, meningiomas, and epithelioid sarcomas (6–10). Recently, frequent and specific inactivating mutations in at least six other SWI/SNF subunits have been identified in a variety of cancers, including ARID1A, ARID1B, ARID2, PBRM1, BRD7, and BRG1 (1, 11). In mouse models, inactivation of *Snf5* leads to rapid development of lethal cancers with 100% penetrance, and

Brg1 haploinsufficient mice are tumor prone, establishing these subunits of the complex as bona fide tumor suppressors (1, 12–17). It is noteworthy that recent exome sequencing of 35 human SNF5-deficient rhabdoid tumors identified a remarkably low rate of mutations, with loss of *SNF5* being essentially the sole recurrent event (18). Indeed, in two of the cancers, there were no other identified mutations. These results suggest that the rapid onset of cancer caused by SNF5 loss is driven not by consequent DNA damage but rather by epigenetic alterations resulting from loss of this chromatin remodeling subunit (18, 19).

Despite substantial effort in recent years, the molecular mechanisms underlying such a wide range of biological functions of Swi/Snf complex remain unclear (20, 21). In vitro studies using reconstituted nucleosomes have shown that the Swi/Snf complex can unwrap, slide, and eject nucleosomes as well as produce DNA loops on the nucleosome surface (22–24). In vivo, the complex was reported to bind preferentially to promoters and other regulatory regions (25). Interestingly, recent studies indicated that ATP-dependent chromatin remodelers are required for establishing the regular nucleosome organization at the 5' end of genes (26). These findings suggest that Swi/Snf complex may affect transcription by mobilizing nucleosomes in promoters and altering accessibility of DNA for transcription factors. However, the extent to which it remodels nucleosomes in vivo and whether it serves any role in the establishment of the canonical nucleosome patterns are unknown.

In this study, we sought to investigate the in vivo functions of the mammalian Swi/Snf complex in the establishment and maintenance of nucleosome landscapes at transcription start sites (TSS). We generated primary mouse cells in which key subunits of the Swi/Snf complex (*Snf5* or *Brg1*) are genetically deleted and compared nucleosome profiles in mutant and WT cells. We also mapped the locations of Swi/Snf complex in WT cells as well as examining the impact of its inactivation on gene expression. Our results show that the complex is essential for the establishment of both occupancy and phasing of the nucleosomes

Author contributions: M.Y.T., C.G.S., P.L., P.J.P., and C.W.M.R. designed research; M.Y.T., C.G.S., P.L., E.C.K., K.C.H., E.J.T., J.A.E., and B.G.W. performed research; M.Y.T., C.G.S., P.L., and B.H.A. contributed new reagents/analytic tools; M.Y.T., C.G.S., P.L., E.C.K., K.C.H., B.H.A., E.J.T., J.A.E., B.G.W., P.J.P., and C.W.M.R. analyzed data; and M.Y.T., C.G.S., P.L., P.J.P., and C.W.M.R. wrote the paper.

The authors declare no conflict of interest.

This article is a PNAS Direct Submission.

Data deposition: The data reported in this paper have been deposited in the Gene Expression Omnibus (GEO) database, www.ncbi.nlm.nih.gov/geo (accession no. GSE46588).

¹M.Y.T., C.G.S., and P.L. contributed equally to this work.

²Present address: Department of Molecular Biology, Massachusetts General Hospital, Boston, MA 02114.

³To whom correspondence may be addressed. E-mail: charles_roberts@dfci.harvard.edu or peter_park@harvard.edu.

This article contains supporting information online at www.pnas.org/lookup/suppl/doi:10.1073/pnas.1302209110/-DCSupplemental.

at a large number of promoters, and that the disruption of the canonical nucleosome patterns at TSS leads to downstream changes in gene expression.

Results

Inactivation of *Swi/Snf* Leads to Reduced Nucleosome Occupancy at Peri-TSS Regions. Nucleosomal profiles at TSS of active genes in mammals consist of a nucleosome-depleted region (NDR) located immediately upstream of the TSS flanked by two well-positioned nucleosomes, referred to as the -1 and $+1$ nucleosomes (27–29) (Fig. 1A). Downstream of the TSS, several additional nucleosomes are also present in stably phased positions. In contrast, silent genes generally lack positioned nucleosomes at TSS, with the exception of a moderately well-positioned nucleosome at the $+1$ position (29). We considered three aspects of nucleosome landscape in the regions surrounding TSS (hereafter referred to as peri-TSS regions) that might be controlled by *Swi/Snf* (Fig. 1A). The first is the positioning of individual nucleosomes relative to the TSS, such as the precisely positioned -1 and $+1$ nucleosomes. The second is nucleosome occupancy, which reflects the frequency with which a nucleosome is present at a particular location within cell population. The third is the presence of regularly spaced nucleosomal arrays, referred to as nucleosome phasing, downstream of the TSS in active promoters.

To examine the *in vivo* functions of *Swi/Snf*, we deleted either *Snf5* or *Brg1* in primary cells. We transduced murine embryonic fibroblasts (MEFs) derived from *Snf5*-conditional (*Snf5*^{f/f}), *Brg1*-conditional (*Brg1*^{f/f}), and control WT mice with retrovirus containing the bacterial Cre recombinase gene, which results in the deletion of the conditionally targeted genes, and achieved nearly complete elimination of *Snf5* or *Brg1* protein (SI Appendix, Fig. S1A and B). We used micrococcal nuclease (MNase) digestion assays to profile nucleosome occupancy in these cells.

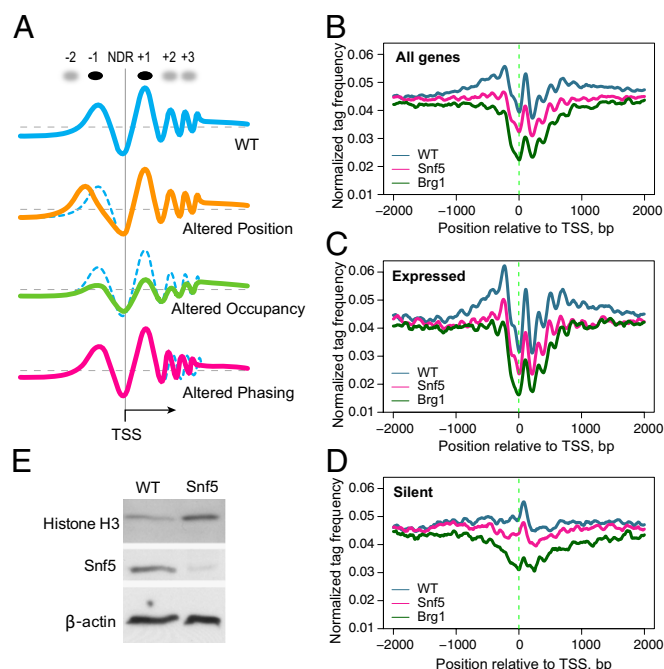


Fig. 1. *Snf5*- and *Brg1*-deficient cells display loss of nucleosome occupancy around the TSS. (A) Key parameters of the nucleosome landscape. We considered the possibility that loss of *Swi/Snf* could affect position (orange line), occupancy (green line), or spacing of phased nucleosomes (pink line). Genomewide nucleosome occupancy profiles at peri-TSS regions are shown for all genes (B), expressed genes (C), and silent genes (D). Profiles for WT and *Snf5*- and *Brg1*-deficient cells are shown with blue, pink, and green lines, respectively. (E) Immunoblot for nonchromatin-associated Histone H3 in WT and *Snf5*-deficient cells.

Because promoters are enriched for easily removable, “fragile” nucleosomes (30–32), we used mild MNase digestion conditions to obtain the most informative nucleosome profiles at these regions. We isolated mononucleosomes (comprising ~10% of entire chromatin) and sequenced the purified DNA on the Helicos platform (*Materials and Methods*). This platform does not require PCR amplification, thus significantly reducing the GC bias (33). This is particularly relevant for our analysis given the affinity bias of nucleosomes for GC-rich sequences (34, 35).

We observed that in WT cells, active genes display high levels of nucleosome occupancy immediately upstream of the NDR with prominent and precisely positioned -1 and $+1$ nucleosomes (Fig. 1B), consistent with previous reports (29). Upon *Snf5* loss, nucleosome occupancy was markedly reduced across the peri-TSS region. In particular, the high nucleosome occupancy upstream of the NDR was completely abolished and the occupancy at the $+1$ nucleosome was substantially reduced. These effects were particularly prominent at expressed genes (Fig. 1C). Interestingly, the positions of the NDR and nucleosomes $+1$ through $+5$ remained roughly the same as in WT cells and were readily identifiable. At silent genes, the changes were similar but less pronounced (Fig. 1D). When *Brg1* was inactivated, nucleosome occupancy was further depleted across the TSS (Fig. 1B–D). The prominent -1 nucleosome position was eliminated and the occupancy of the $+1$ position was severely reduced such that its peak was even below baseline occupancy levels distant from the TSS. When individual genes were examined, similar effects were observed but with considerable diversity, indicating that the genes were not uniformly affected (SI Appendix, Fig. S2A, D, and E).

We next examined whether the alteration in nucleosome occupancy was dependent upon promoter type, CpG island (CpGi)-containing versus non-CpGi, because analysis of *Brg1* shRNA knock-down in macrophages concluded that CpGi-containing genes were largely *Swi/Snf*-independent (36). We observed that inactivation of *Snf5* or *Brg1* led to a marked reduction in nucleosome occupancy at both CpGi and non-CpGi promoters (SI Appendix, Fig. S3), suggesting that, at least in MEFs, the *Swi/Snf* complex contributed the establishment of nucleosome occupancy profiles at both types of promoters. When genes were further stratified by expression status in addition to the presence of CpGi, *Swi/Snf* inactivation led to reduced peri-TSS occupancy, particularly at the -1 and $+1$ nucleosomes in all subclasses.

We also performed a number of checks to ensure that the observed differences in the nucleosome occupancy between WT and mutant samples did not originate from experimental or data processing artifacts. In particular, to confirm that the observed defects in *Snf5*- and *Brg1*-deficient cells were not due to their inability to express histones, we measured total nonchromatin-associated histone H3 in WT and *Snf5*-deficient cells by immunoblotting. *Snf5*-deficient cells displayed increased levels of unincorporated histone H3, suggesting that impaired deposition of nucleosomes resulted in an increase in the pool of free histones (Fig. 1E). We also repeated the nucleosome profiling experiments using the Illumina platform for two concentrations of MNase (SI Appendix, Fig. S4). With paired-end sequencing, we verified that the distributions of the nucleosome fragment sizes were similar for all samples at each MNase concentration (SI Appendix, Fig. S4A and B), which is indicative of the same level of digestion (37). We observed that the TSS profiles were similar for the WT and mutant samples in the case of the light digestion (SI Appendix, Fig. S4C). At the moderate digestion level, however, the occupancy at TSS decreased substantially in the mutant cells compared with the WT, consistent with our Helicos data (SI Appendix, Fig. S4D). Furthermore, we analyzed data from a recent independent study that evaluated the role of *Brg1* in differentiation using human CD36⁺ cells (38) and found a similar decrease in nucleosome occupancy at TSS induced by *Brg1* inactivation (SI Appendix, Fig. S4F). Based on these observations, we conclude that *Swi/Snf* inactivation leads to reduction of nucleosome occupancy at a substantial fraction of promoters of diverse types.

Inactivation of Swi/Snf Results in Altered Nucleosome Phasing. Previous studies have shown that ATP-dependent chromatin remodelers can modulate the spacing between individual nucleosomes and that even subtle changes in linker lengths can substantially affect transcription factor binding (38). We sought to evaluate whether the Swi/Snf complex also contributes to the internucleosomal spacing. We found that the position of the +1 nucleosome remained constant in all cell types, but the phasing of nucleosomes downstream of the +1 position (+2, +3, and +4) was altered, with a slight shift toward the TSS (Fig. 2A). To quantify this change, we performed Fourier analysis, which is often used to quantify the changes in nucleosome phasing (39). This analysis revealed that the average internucleosomal distance of 182 bp in peri-TSS regions in WT MEFs was reduced to 174 bp in both *Snf5*- and *Brg1*-deficient cells (Fig. 2B). Thus, our results indicate that in addition to the regulation of nucleosome occupancy, the Swi/Snf complex affects nucleosome phasing in the peri-TSS region in vivo.

Swi/Snf Binds to a Subset of Promoters and Controls Nucleosome Occupancy. Given the marked effect of *Snf5* and *Brg1* loss on the nucleosome landscape at promoters, we sought to determine the localization of Swi/Snf and to classify genes based upon the degree of Swi/Snf binding. We performed *Brg1* ChIP combined with MNase digestion to achieve nucleosome-resolution mapping of the complex (40). Consistent with a prior report (25), *Brg1* preferentially bound promoter regions and the level of binding was positively correlated with expression level of the target genes ($R = 0.55$, Fig. 3A). Although binding was greatest at the +1 nucleosome position, we found that *Brg1* was also enriched at the NDR.

Across the genome, *Brg1* enrichment at peri-TSS regions in WT cells exhibited a bimodal distribution, indicating clear binding at a subset of promoters and low or no binding at the rest (Fig. 3B). For the subset of genes with high *Brg1* enrichment, the nucleosome profile displayed prominent occupancy at the -1 and +1 positions, a pronounced NDR and readily identifiable nucleosome phasing (Fig. 3C). In contrast, the average occupancy profile for genes with low *Brg1* enrichment was nearly flat, except for a slight increase at the +1 position (Fig. 3D). The two groups also differed in composition: genes with high levels of *Brg1* binding were enriched for CpGs, whereas the majority of genes with low levels of *Brg1* binding lacked CpGs (75% vs. 20%; *SI Appendix, Table S1*). Furthermore, although the loss of *Brg1* led to reduced nucleosome occupancy at TSS region in both groups, we found that higher levels of *Brg1* enrichment indeed correlated with a greater degree of nucleosome depletion following *Brg1* deletion ($R = -0.32$, $P < 10^{-32}$; *SI Appendix, Figs. S2 B and C and S5*). Collectively, these findings strongly suggest that the loss of nucleosome occupancy at TSS in the mutant cells is a direct rather than secondary effect of Swi/Snf inactivation.

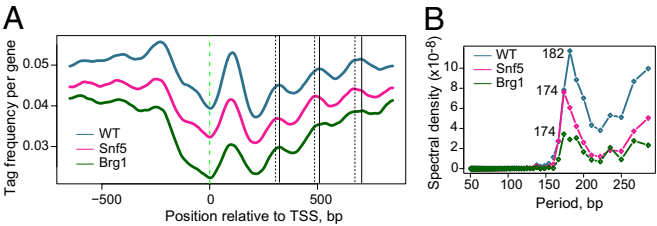


Fig. 2. *Snf5*- and *Brg1*-deficient cells display altered nucleosomal phasing. (A) Alignment of WT, *Snf5*-deficient, and *Brg1*-deficient nucleosomal profiles. Thin vertical lines mark stable nucleosome positions in WT (solid lines) and *Snf5* mutant cells (dotted lines). (B) Fourier analysis reveals internucleosomal distance of 182 bp in WT cells (blue line) and 174 bp in *Snf5*- and *Brg1*-deficient cells (pink and green lines, respectively).

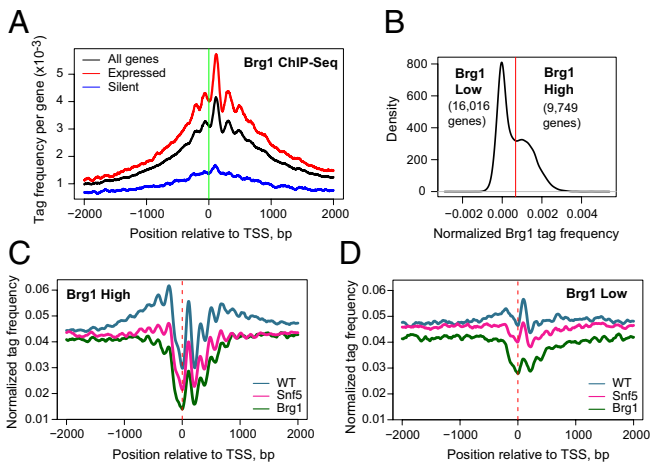


Fig. 3. *Brg1* ChIP reveals enrichment of Swi/Snf at peri-TSS regions. (A) *Brg1* binding is prominent at TSS. Results are shown for all (black), expressed (red), and silent (blue) genes. (B) *Brg1* enrichment in the TSS region (+/-2 kb) displays a bimodal distribution. The red line indicates the threshold of *Brg1* enrichment used to identify groups of genes with low and high *Brg1* levels. (C and D) Nucleosomal occupancy profiles for *Brg1* high and *Brg1* low genes.

Effect of *Snf5*/*Brg1* Inactivation on Gene Expression. To determine how changes in nucleosome occupancy driven by inactivation of *Snf5* or *Brg1* affect gene expression, we profiled mRNAs from the same samples on Affymetrix microarrays. Overall, changes in gene expression were relatively modest and variable in magnitude and direction for individual genes, and most genes had similar expression levels in mutant and WT cells. However, a subset of genes displayed altered expression (*SI Appendix, Fig. S6 A and B*), with more genes being significantly up-regulated than down-regulated (793 vs. 491 following *Snf5* loss, and 1,226 vs. 782 genes following *Brg1* loss; $P < 0.01$ in both cases, Fisher's exact test). There was a high degree of overlap between the genes affected by *Snf5* loss and those affected by *Brg1* loss (Table 1 and *SI Appendix, Figs. S7 and S8 A–D*), suggesting similar but not identical impact in the two cases. Overall, we observed a low but statistically significant negative correlation between gene expression and level of nucleosome occupancy at the NDR in both WT and mutant MEFs (*SI Appendix, Fig. S9 A–C*). When we examined the relationship between changes in nucleosome occupancy and changes in gene expression caused by *Snf5* or *Brg1* loss, there was only a modest association between greater increase in nucleosome occupancy with stronger gene down-regulation and vice versa (*SI Appendix, Figs. S8 E–H and S9 D and E*). These findings suggest that the average transcription rate at the majority of genes is maintained even when nucleosome occupancy is altered around the TSS. It is noteworthy that similar findings have been made recently in yeast, where inactivation of related chromatin remodelers revealed that changes in nucleosome organization did not correlate with changes in transcription (41).

Table 1. Relationship between the sets of genes up- or down-regulated in the absence of *Snf5* or *Brg1*

Gene set	<i>Brg1</i> up	<i>Brg1</i> no change	<i>Brg1</i> down
<i>Snf5</i> up	510	272	6
<i>Snf5</i> no change	710	10,410	454
<i>Snf5</i> down	1	168	322

Numbers of genes in each overlapping group are shown. The table cells corresponding to up- and down-regulated genes are shaded in pink and blue, respectively.

To examine whether there existed specific features of nucleosome organization that may play a role in regulating gene expression, we examined the relative nucleosome density at different positions near the TSS, which has been shown to correlate with transcription rate (42, 43). For example, a high level of transcription correlates with high relative occupancy at the -1 and $+1$ positions accompanied by low occupancy at the NDR. To quantify such effects, we calculated a “relative occupancy score” by subtracting occupancy at the NDR from occupancy at the -1 and $+1$ positions and normalizing it by the baseline tag density for each TSS (Fig. 4A; *Materials and Methods*). In WT cells, higher relative occupancy scores were found in genes that had higher expression levels. These include gene sets that have CpGs in their promoters as well as those having high Brg1 binding (SI Appendix, Fig. S10A). This finding confirms that a pronounced pattern of NDR flanked by two positioned nucleosomes (high score) correlates with high level of expression.

For the *Snf5*^{−/−} and *Brg1*^{−/−} samples, a significant reduction in the score was observed compared with the WT samples (Fig. 4B, $P < 10^{-30}$). This suggests a complex relationship with two seemingly opposing effects of Swi/Snf inactivation. On the one hand, subunit inactivation results in a decrease in overall nucleosome occupancy at the TSS (Fig. 1), which would be predicted to correlate with up-regulation. On the other hand, it results in a reduction in relative occupancy at the -1 and $+1$ nucleosomes (Fig. 4), which would be predicted to correlate with down-regulation. Moreover, although actively expressed genes exhibit significantly higher scores than silent genes on average (SI Appendix, Fig. S10A), changes in the relative and absolute occupancy at TSS were poorly correlated at the individual gene level ($|R| < 0.1$ for both mutant samples; SI Appendix, Fig. S10B and C). In facilitating coordinated gene expression responses such as during differentiation, the Swi/Snf complex has been shown capable of interacting with both coactivators and corepressors. Consequently, expression changes at individual genes may depend upon whether the gene is normally bound predominantly by activators or repressors.

Because the effect of Brg1 inactivation might be either activating or repressive, we next evaluated whether enrichment in Brg1 correlates with the magnitude of change in gene expression without accounting for the direction of this change. We observed that the genes with high Brg1 enrichment displayed significantly larger absolute change in expression than genes with low levels of Brg1 enrichment (Fig. 4C). In comparison, when direction of the expression change was considered, this difference was considerably reduced (SI Appendix, Fig. S10D). Although modest in magnitude, the mean change was again significantly greater than zero ($P < 0.023$) for genes highly enriched for Brg1, indicating that Brg1 loss slightly favored activation over repression, consistent with the overall effects we identified on gene expression.

Functions Regulated by Swi/Snf. Identification of the genes that are regulated by Swi/Snf in MEFs allowed us to investigate whether specific cellular functions or pathways were affected by Swi/Snf

mutation. Genes up-regulated in the absence of Snf5 demonstrated enrichment for four Gene Ontology (GO) sets ($P < 0.01$): cell-cycle process, cell-cycle phase, mitotic cell cycle, and cell division (SI Appendix, Table S2). Brg1 loss yielded a larger number of up-regulated gene sets, but the same theme emerged, with the top 5 and 21 of the 67 gene sets specific for cell-cycle progression. For the genes down-regulated following Snf5 loss, no annotated gene sets were significant. For Brg1 loss, down-regulated genes were significantly enriched for 20 gene sets, several of which were associated with extracellular interactions and motility. Thus, our findings indicate that the loss of Swi/Snf complex primarily results in stimulation of cell proliferation pathways, consistent with the links between Swi/Snf mutation and tumorigenesis.

Discussion

Our data demonstrate that the Swi/Snf complex serves specific roles in vivo in establishing and defining the nucleosome landscape at target promoters. Specifically, we find that the complex is highly enriched not only at the -1 and $+1$ positions, but also over the NDR where there is a paucity of nucleosomes. We further show that the complex is essential for broad establishment of high levels of nucleosome occupancy across target promoters relative to their flanking regions.

In principle, there is a possibility that the complex affects nucleosome occupancy at TSS through secondary effects (e.g., mediated by expression changes). However, our observation of strong correlation between the presence of the complex and its effect on nucleosome occupancy at promoters (Fig. 3) as well as high similarity of the differentially expressed gene lists in Snf5- and Brg1-deficient cells (Table 1 and SI Appendix, Figs. S7 and S8) argue in favor of the direct involvement of the complex. Consequently, activity of the complex is quite specific in that it serves to sculpt the landscape at active promoters by building occupancy at the -1 and $+1$ positions while ensuring relative depletion of nucleosomes at the NDR to establish the classic high peaks and low trough landscape (Fig. 5). Our study is focused upon nucleosomes easily released with MNase; thus, changes in chromatin structure that decrease accessibility or increase stability of nucleosomes in peri-TSS regions could, in principle, contribute to the observed differences. Although we cannot completely exclude at least a partial contribution of such a mechanism, this scenario seems unlikely given the positive correlation between the observed effect and transcription activity (SI Appendix, Fig. S9D and E). We also note that the sequencing depth achieved in this study allows making confident conclusions about influence of Swi/Snf complex on average for a large set of genes but not for individual genes; variability of the Swi/Snf effects at the individual gene level may be substantial.

Nucleosome sliding *in cis* and nucleosome transfer have been identified as the main or sole activities of the Swi/Snf complex in a number of studies (23, 44–46). Importantly, despite the ability of the complex to slide nucleosomes *in vitro*, our data demonstrate that it appears to have no role in establishing the positions of the major TSS-flanking -1 and $+1$ nucleosomes. Although deletion of the complex subunits results in reduction of occupancy at these positions, the peaks remain sharp, indicating that the residual nucleosomes are well positioned and unchanged in location. Given the overall reduction in occupancy, these findings suggest that transfer of nucleosomes onto DNA is the principal mechanism of action for the Swi/Snf complex at these positions. However, downstream of the $+1$ position, Swi/Snf is likely to contribute to the phasing via a sliding activity and/or affecting “statistical” nucleosome positioning (27), as evidenced by subtle alterations in nucleosome spacing there. This is also supported by a recent study showing that the yeast Swi/Snf complex can bind and shift promoter nucleosomes away from the TSS (47), although no pronounced loss of nucleosome occupancy upon Swi/Snf perturbation was reported there. Whether this reflects a functional difference between yeast and mammalian Swi/Snf complexes is unclear. Further studies are warranted to address this question. In addition, SWI/SNF effects may vary

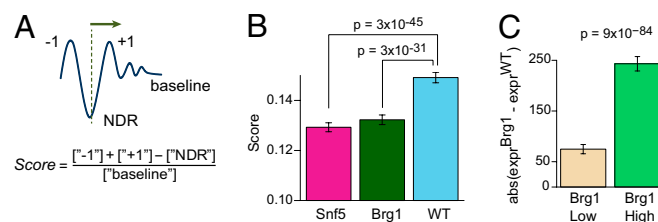


Fig. 4. Effects of nucleosome occupancy and Brg1 binding on transcription. (A) Schematic illustration of the relative nucleosome occupancy score definition. (B) Comparison of the score in WT (blue), Snf5 (pink), and Brg1 (green) samples. (C) Average absolute changes in gene expression upon Brg1 inactivation are compared for genes with low and high Brg1 enrichment. The 95% confidence intervals and P values are indicated.

Downloaded by guest on February 26, 2022

then isolated, end-repaired, and treated with Taq polymerase to generate a protruding A base for adaptor ligation. After ligation of a pair of Illumina adaptors, the DNA was size selected and amplified by PCR using the adaptor primers. The amplified DNA was then purified and used for cluster generation and sequencing.

Histone Solubility. To evaluate total nonchromatin-associated histone H3 in WT and Snf5-deficient cells, equal numbers of nuclei were isolated by centrifugation through a sucrose gradient (as described in the preparation of mononucleosomes). Nuclei were then resuspended for 10 min in ice-cold Buffer 4 (0.32 M sucrose, 50 mM Tris pH 7.6, 4 mM MgCl₂, 1 mM CaCl₂, protease inhibitors) containing a final concentration of 1% (vol/vol) Nonidet P-40. The extract was then spun at 10,000 × g in a refrigerated microcentrifuge. Supernatants containing nonchromatin-associated proteins were run on SDS/PAGE and immunoblotted for Histone H3 (Abcam), Snf5 (Bethyl), and Actin (Sigma).

Brg1 ChIP. Nuclei from WT MEFs were isolated and subjected to micrococcal nuclease digestion followed by brief sonication to release nucleosomal fragments. Brg1 ChIP was performed on the lysate and immunoprecipitated DNA was purified and sequenced.

Data Analysis. A detailed description of the computational methods is provided in the *SI Appendix*. In brief, sequenced tags were mapped to the mm9

assembly of the mouse genome. Tags were filtered for possible artifacts before further analyses. The final tag counts for the data sets used in this study are summarized in *SI Appendix, Table S3*. The coordinates of genes and CpGs were taken from the University of California Santa Cruz annotations. Gene expression data were generated on GeneChip Mouse Genome 430A 2.0 Arrays (Affymetrix) and processed using the MAS 5.0 algorithm as implemented in the bioconductor package Affy (www.bioconductor.org). Different background correction and normalization methods were explored (e.g., robust multiarray analysis, quantile normalization) to ensure robustness of the results. The Gene Ontology Term Finder Web server (<http://go.princeton.edu/cgi-bin/GOTermFinder/GOTermFinder>) was used for gene ontology analysis.

ACKNOWLEDGMENTS. We thank Xi Wang for critical review of the manuscript and Lee Whale for the artwork in Figs. 1A and 5. This work was supported in part by a Ruth L. Kirschstein National Research Service Award Fellowship 5F32 CA123776 from the National Cancer Institute (to C.G.S.), U01HG004258 (to M.Y.T.), R01GM082798 (to P.J.P.), R01CA113794 (to C.W.M.R.); an Innovative Research Grant from Stand Up 2 Cancer (to C.W.M.R.); and a U01 NCI Mouse Models of Cancer Consortium Award (to C.W.M.R.). The Sloan Research Fellowship (P.J.P.), Garrett B. Smith Foundation, Miles for Mary, and the foundation Cure AT/RT Now (C.W.M.R.) provided additional support.

- Wilson BG, Roberts CW (2011) SWI/SNF nucleosome remodellers and cancer. *Nat Rev Cancer* 11(7):481–492.
- Reisman D, Glaros S, Thompson EA (2009) The SWI/SNF complex and cancer. *Oncogene* 28(14):1653–1668.
- Weissman B, Knudsen KE (2009) Hijacking the chromatin remodeling machinery: Impact of SWI/SNF perturbations in cancer. *Cancer Res* 69(21):8223–8230.
- Narlikar GJ, Fan HY, Kingston RE (2002) Cooperation between complexes that regulate chromatin structure and transcription. *Cell* 108(4):475–487.
- Martens JA, Winston F (2003) Recent advances in understanding chromatin remodeling by Swi/Snf complexes. *Curr Opin Genet Dev* 13(2):136–142.
- Biegel JA, et al. (1999) Germ-line and acquired mutations of INI1 in atypical teratoid and rhabdoid tumors. *Cancer Res* 59(1):74–79.
- Versteeg I, et al. (1998) Truncating mutations of hSNF5/INI1 in aggressive paediatric cancer. *Nature* 394(6689):203–206.
- Hulsebos TJ, et al. (2007) Germline mutation of INI1/SMARCB1 in familial schwannomatosis. *Am J Hum Genet* 80(4):805–810.
- Christiaans I, et al. (2011) Germline SMARCB1 mutation and somatic NF2 mutations in familial multiple meningiomas. *J Med Genet* 48(2):93–97.
- Modena P, et al. (2005) SMARCB1/INI1 tumor suppressor gene is frequently inactivated in epithelioid sarcomas. *Cancer Res* 65(10):4012–4019.
- Garraway LA, Lander ES (2013) Lessons from the cancer genome. *Cell* 153(1):17–37.
- Bultman SJ, et al. (2008) Characterization of mammary tumors from Brg1 heterozygous mice. *Oncogene* 27(4):460–468.
- Roberts CW, Galusha SA, McMenamin ME, Fletcher CD, Orkin SH (2000) Haploinsufficiency of Snf5 (integrase interactor 1) predisposes to malignant rhabdoid tumors in mice. *Proc Natl Acad Sci USA* 97(25):13796–13800.
- Roberts CW, Leroux MM, Fleming MD, Orkin SH (2002) Highly penetrant, rapid tumorigenesis through conditional inversion of the tumor suppressor gene Snf5. *Cancer Cell* 2(5):415–425.
- Klochendler-Yeivin A, et al. (2000) The murine SNF5/INI1 chromatin remodeling factor is essential for embryonic development and tumor suppression. *EMBO Rep* 1(6):500–506.
- Guidi CJ, et al. (2001) Disruption of Ini1 leads to peri-implantation lethality and tumorigenesis in mice. *Mol Cell Biol* 21(10):3598–3603.
- Tsikitis M, Zhang Z, Edelman W, Zagzag D, Kalpana GV (2005) Genetic ablation of Cyclin D1 abrogates genesis of rhabdoid tumors resulting from Ini1 loss. *Proc Natl Acad Sci USA* 102(34):12129–12134.
- Lee RS, et al. (2012) A remarkably simple genome underlies highly malignant pediatric rhabdoid cancers. *J Clin Invest* 122(8):2983–2988.
- McKenna ES, et al. (2008) Loss of the epigenetic tumor suppressor SNF5 leads to cancer without genomic instability. *Mol Cell Biol* 28(20):6223–6233.
- Clapier CR, Cairns BR (2009) The biology of chromatin remodeling complexes. *Annu Rev Biochem* 78:273–304.
- Liu N, Balliano A, Hayes JJ (2011) Mechanism(s) of SWI/SNF-induced nucleosome mobilization. *ChemBioChem* 12(2):196–204.
- Lorch Y, Maier-Davis B, Kornberg RD (2010) Mechanism of chromatin remodeling. *Proc Natl Acad Sci USA* 107(8):3458–3462.
- Kassabov SR, Zhang B, Persinger J, Bartholomew B (2003) SWI/SNF unwraps, slides, and rewraps the nucleosome. *Mol Cell* 11(2):391–403.
- Dechassa ML, et al. (2010) SWI/SNF has intrinsic nucleosome disassembly activity that is dependent on adjacent nucleosomes. *Mol Cell* 38(4):590–602.
- Ho L, et al. (2009) An embryonic stem cell chromatin remodeling complex, esBAF, is essential for embryonic stem cell self-renewal and pluripotency. *Proc Natl Acad Sci USA* 106(13):5181–5186.
- Zhang Z, et al. (2011) A packing mechanism for nucleosome organization reconstituted across a eukaryotic genome. *Science* 332(6032):977–980.
- Jiang C, Pugh BF (2009) Nucleosome positioning and gene regulation: Advances through genomics. *Nat Rev Genet* 10(3):161–172.
- Hartley PD, Madhani HD (2009) Mechanisms that specify promoter nucleosome location and identity. *Cell* 137(3):445–458.
- Schones DE, et al. (2008) Dynamic regulation of nucleosome positioning in the human genome. *Cell* 132(5):887–898.
- Henikoff S, Henikoff JG, Sakai A, Loeb GB, Ahmad K (2009) Genome-wide profiling of salt fractions maps physical properties of chromatin. *Genome Res* 19(3):460–469.
- Weiner A, Hughes A, Yassour M, Rando OJ, Friedman N (2010) High-resolution nucleosome mapping reveals transcription-dependent promoter packaging. *Genome Res* 20(1):90–100.
- Xi Y, Yao J, Chen R, Li W, He X (2011) Nucleosome fragility reveals novel functional states of chromatin and poises genes for activation. *Genome Res* 21(5):718–724.
- Goren A, et al. (2010) Chromatin profiling by directly sequencing small quantities of immunoprecipitated DNA. *Nat Methods* 7(1):47–49.
- Peckham HE, et al. (2007) Nucleosome positioning signals in genomic DNA. *Genome Res* 17(8):1170–1177.
- Kharchenko PV, Woo CJ, Tolstorukov MY, Kingston RE, Park PJ (2008) Nucleosome positioning in human HOX gene clusters. *Genome Res* 18(10):1554–1561.
- Ramirez-Carrozzi VR, et al. (2009) A unifying model for the selective regulation of inducible transcription by CpG islands and nucleosome remodeling. *Cell* 138(1):114–128.
- Johnson SM, Tan FJ, McCullough HL, Riordan DP, Fire AZ (2006) Flexibility and constraint in the nucleosome core landscape of *Caenorhabditis elegans* chromatin. *Genome Res* 16(12):1505–1516.
- Hu G, et al. (2011) Regulation of nucleosome landscape and transcription factor targeting at tissue-specific enhancers by BRG1. *Genome Res* 21(10):1650–1658.
- Wang J, et al. (2012) Sequence features and chromatin structure around the genomic regions bound by 119 human transcription factors. *Genome Res* 22(9):1798–1812.
- He HH, et al. (2010) Nucleosome dynamics define transcriptional enhancers. *Nat Genet* 42(4):343–347.
- Gkikopoulos T, et al. (2011) A role for Snf2-related nucleosome-spacing enzymes in genome-wide nucleosome organization. *Science* 333(6050):1758–1760.
- Tirosh I, Barkai N (2008) Two strategies for gene regulation by promoter nucleosomes. *Genome Res* 18(7):1084–1091.
- Batta K, Zhang Z, Yen K, Goffman DB, Pugh BF (2011) Genome-wide function of H2B ubiquitylation in promoter and genic regions. *Genes Dev* 25(21):2254–2265.
- Whitehouse I, et al. (1999) Nucleosome mobilization catalysed by the yeast SWI/SNF complex. *Nature* 400(6746):784–787.
- Gutiérrez JL, Chandy M, Carrozza MJ, Workman JL (2007) Activation domains drive nucleosome eviction by SWI/SNF. *EMBO J* 26(3):730–740.
- Lorch Y, Cairns BR, Zhang M, Kornberg RD (1998) Activated RSC-nucleosome complex and persistently altered form of the nucleosome. *Cell* 94(1):29–34.
- Yen K, Vinayachandran V, Batta K, Koerber RT, Pugh BF (2012) Genome-wide nucleosome specificity and directionality of chromatin remodelers. *Cell* 149(7):1461–1473.
- Lomvardas S, Thanos D (2001) Nucleosome sliding via TBP DNA binding in vivo. *Cell* 106(6):685–696.
- Thurman RE, et al. (2012) The accessible chromatin landscape of the human genome. *Nature* 489(7414):75–82.
- Prochasson P, Neely KE, Hassan AH, Li B, Workman JL (2003) Targeting activity is required for SWI/SNF function in vivo and is accomplished through two partially redundant activator-interaction domains. *Mol Cell* 12(4):983–990.
- Wang X, et al. (2009) Oncogenesis caused by loss of the SNF5 tumor suppressor is dependent on activity of BRG1, the ATPase of the SWI/SNF chromatin remodeling complex. *Cancer Res* 69(20):8094–8101.
- Isakoff MS, et al. (2005) Inactivation of the Snf5 tumor suppressor stimulates cell cycle progression and cooperates with p53 loss in oncogenic transformation. *Proc Natl Acad Sci USA* 102(49):17745–17750.